Chemical and Materials Engineering 2(8): 173-178, 2014
DOI: 10.13189/cme.2014.020802 http://www.hrpub.org

Preparation and Characterization of Silver/Organo-clay Nanocomposites

Natália Fernanda Nunes Pessanha[1], Kátia Yuri Fausta Kawase[2], Gerson Luiz Vieira Coelho[1,*]

[1]Laboratory of Separation Processes, Department of Chemical Engineering, Federal Rural University of Rio de Janeiro, Brazil
[2]Fluminense Federal Institute of Education, Science and Technology, Brazil

Abstract This study investigated the application of organo-clay as a support in the synthesis of silver nanoparticles with increased antimicrobial activity – the Ag-montmorillonite nanocomposite (Ag-MMT). This technology is utilized to improve the antibacterial function of materials, especially those used in polymeric nanocomposites. This purpose fulfils the recently increasing public concerns on hygiene and brings solutions to health, safety, and microbial protection. The experimental steps consisted of purification with hydrogen peroxide to remove organic matter and modification with Cetyl trimethyl ammonium bromide to increase basal spacing in the clay. The purified Ag-MMT nanocomposites were obtained from organo-clay and silver nitrate ($AgNO_3$) as the silver precursor in the concentrations of 0.005 M, 0.01 M, 0.02 M, 0.05 M, and 0.1 M. The nanocomposites' properties were analyzed as a function of the sodium borohydride ($NaBH_4$) concentration, the reducing agent. The X-ray diffraction analysis showed that the structure of the purified MMT was gradually exfoliated with increasing concentrations of $AgNO_3$ while the organo-clay structure remained intact. Samples of Ag^+-MMT were reduced with $NaBH_4$ to produce Ag^o; the UV-vis spectra showed which particle diameters were dependent on the $NaBH_4$ concentration. The Ag-MMT organo-clay nanocomposite showed the highest antimicrobial activity against *Escherichia coli* as the result of its high concentration of silver nanoparticles.

Keywords Adsorption, Ag, Organo-clay, Nanoscale

1. Introduction

The oligodynamic activity of even low concentrations of silver (Ag) has been recognized as negatively affecting living organisms since ancient times. The use of silver as an antimicrobial material is attractive because silver has the highest degree of toxicity to more than 650 pathogenic microorganisms but low toxicity to animal cells. The antimicrobial activity of silver is enhanced when silver is in the colloidal form, i.e. in the nanometer size (size ranging from 10^{-9} m to 10^{-6} m). Thus, nano silver provides an increased number of particles per unit area [1-3]. Silver-based compounds have been extensively used in many industrial applications, such as in fabrics antimicrobial dressings, curatives, catheters, water filtration systems, and food packing containers, to prevent the proliferation of microorganisms.

Silver nanoparticles can be synthesized through several routes, however, the most commonly used means of reducing silver ions for the production of nanocomposites are γ irradiation [4], UV irradiation [5,6], thermal reduction [7,8], and application of chemical reducers such as N,N-dimethylformamide [9], ethylene glycol [10], sodium borohydride [11-13], sodium citrate [14], ascorbic acid [15], and formaldehyde [16] among others.

Chemical reduction generally uses strong reducing agents, e.g. $NaBH_4$, that serve as stabilizing agents that simultaneously reduce the tendency of nanoparticles to aggregate in solution. According to [17], $NaBH_4$ provides a surface charge on particles that keep them in suspension by electrostatic repulsive forces. Inorganic polymeric compounds or solid surfaces such as glass and kaolinite and montmorillonite phyllosilicates are used to stabilize dispersion and diameters of synthesized nanoparticles.

Studies on production of Ag-nanocomposites usually focus on steric stabilization, which is the introduction of long molecular chains on the particles' surfaces to limit their approximation in solution. Inorganic stabilizers such as amines, thiols, acids, and alcohols can be used in the synthesis of silver nanoparticles. Polymeric compounds such as polyvinylpyrrolidone, polyvinyl alcohol, polyethylene glycol, polyethylene phthalate, and copolymers among others have been described as effective stabilizers. Nanocomposites formed by polymers and inorganic particles generally exhibit individual particles that can be of unequal sizes (polydisperse) or agglomerated in clusters [18].

The synthesis of metal nanoparticles on solid supports such as smectite clays is a suitable form to control particle size. The montmorillonite clay (MMT) has a lamellar structure, swelling capacity in aqueous media, and cation

exchange capacity. The lamellar surface has charge-compensating cations (Ca^{2+}, Na^{+} and Li^{+}) that are substituted by other metallic ions. The reduction in these metal ions leads to nanosized particles because the lamellar spacing serves as a nanoreactor limiting the particles' size; thus, agglomeration is prevented and optimal dispersion of particles on the clay surface is ensured [19].

Because of the reported antimicrobial activity of Ag-MMT nanocomposites, this study aimed at synthesizing silver nanoparticles in organo-clay to evaluate if increases in its basal spacing with a quaternary salt could increase its capacity for metallic silver adsorption and, therefore, expand its biocide activity against *Escherichia coli*.

2. Materials and Methods

2.1. Reagents

The commercial sodium bentonite clay (Argel CN 35) used in the study, codified as MMT, was provided by the branch of the Bentonit Northeastern Union S.A. located in São Paulo - SP. This sodium bentonite clay has a cation exchange capacity (CEC) of 100 meq/100 g and a particle size of 200 mesh. The following analytical grade reagents were purchased from Vetec Chemistry Ltd.: hydrogen peroxide (H_2O_2), organic modifier cetyl trimethyl ammonium bromide commercially known as Cetremide® ($C_{19}H_{42}BrN$; HDTMABr), silver nitrate ($AgNO_3$) and sodium borohydride ($NaBH_4$). Deionized water was used in the preparation of all solutions.

2.2. Clay Purification

The clay was pretreated with 30% hydrogen peroxide for 24 hours in the ratio of 20 mL H_2O_2 per g of dry clay to remove organic contaminants. Excess peroxide was removed through thermostatic heating at 80 °C [20]. The purified clay was suspended in deionized water, vigorously stirred with a magnetic stirrer, and allowed to settle; water was siphoned off and the clay was dried in an oven at 60 ºC for 24 hours.

2.3. Clay Modification

According to [21], quaternary salts should only be added in an amount corresponding to the amount of the clay's cation exchange capacity because salt excess may be retained in the clay. Therefore, the modification process consisted in preparing a suspension containing 30 g of purified clay, the calculated mass of Cetremide quaternary salt, and deionized water; the suspension was stirred for 24 hours. The organo-clay (organophilic MMT) was filtered, washed twice with deionized water, dried in an oven at 60 °C for 24 hours, and stored in amber bottles for later use [22].

2.4. Adsorption Procedure

The adsorption process was carried out in batch and complete darkness to avoid the photoreduction of silver ions. According to the procedure described in [13], 0.2 g (± .0001) of purified clay/organo-clay was weighed on an analytical balance and added to flasks containing 200 mL of $AgNO_3$ solution at concentrations of 0.005 M, 0.01 M, 0.02 M, 0.05 M, and 0.1 M. The flasks were sealed and shaken at 130 rpm, at room temperature, for 24 hours. The suspensions were centrifuged for 20 minutes at 5000 min^{-1} and vacuum filtered through 1.2 μm glass fiber filters (Whatman). The clay was gradually dried at 50 °C for 24 hours. The purified and organophilic montmorillonite clays containing silver ions were labeled Ag^{+}-MMT purif. and Ag^{+}-MMT org., respectively.

$AgNO_3$ solutions were used at different concentrations to evaluate the behavior of the clay's structure and surface.

2.5. Reduction Procedure

One $AgNO_3$ solution concentration was selected as ideal (0.01 M $AgNO_3$) based on the results obtained in the previous procedure. Silver ions present in the Ag^{+}-MMT purif. and Ag^{+}-MMT org. samples were reduced with $NaBH_4$ to obtain the montmorillonite clay impregnated with nanometric metallic silver (Ag-MMT purif. and Ag-MMT org.). Freshly prepared $NaBH_4$ solutions at concentrations of 0.001 M, 0.005 M, and 0.01 M were added to flasks containing Ag^{+}-MMT purif. and Ag^{+}-MMT org. under continuous stirring for a few minutes. After reduction, the Ag-MMT purif. and Ag-MMT org. solutions were vacuum filtered through 1.2 μm fiber glass filters (Whatman) and washed several times with deionized water to remove residual Ag^{+} ions. The residual supernatants (colloids of silver nanoparticles) were analyzed by UV-visible spectrophotometry [11,13,16].

2.6. Characterization

2.6.1. Fourier Transform Infrared – FTIR

Infrared spectroscopy (FT-IR Perkin Elmer Spectrum 100) with wavelengths of 400-4000 cm^{-1} was used to investigate structural changes resulting from alterations in the clay mineral of the modified and unmodified clays.

2.6.2. X-ray diffraction (XRD)

X-ray Diffraction (XRD) analyses were performed using a Rigatu Miniflex Diffraction patterns were taken at room temperature under constant conditions: 40 kV, 30 mA, range of 0.02°, and scans from 2-30° for clays and 2-55° for samples, with silver adsorbed in the clays. Basal spacing (d_{001}) was calculated using Bragg's Law:

$$n\lambda = 2d_0 \quad (1)$$

Where θ is the angle of diffraction, λ is the wavelength (0.15418 nm), and n is the order of diffraction equal to one [19]. The average crystallite size of silver, D, was calculated using the Scherrer equation:

$$D = k\lambda / \beta cos\theta \quad (2)$$

Where the constant k is given the value equal to one, and the β parameter corresponds to the measurement of the width of 2θ diffraction peak at the point where the intensity falls to half. The reflection peak of silver in the crystallographic plane (111) was used, and it was assumed that crystallites have a spherical shape. The β parameter corresponds to the measurement of the width of 2θ diffraction peak at the point where the intensity falls to half (FWHM - full width at half maximum) [11,23].

2.6.3. UV-visible Spectrophotometry

The UV absorption spectra of colloids in the silver nanoparticles resulting from the reduction process were measured with a visible spectrophotometer (BEL Photonics 1105). All spectra were recorded using wavelengths in the range between 320-600 nm and 1 cm wide quartz cuvettes; deionized water was used as blank.

2.7. Antibacterial Activity Assay

The Gram negative pathogen *Escherichia coli* (*E.coli*) was obtained from the microorganisms collection in the Microbiology Laboratory at the DTA/IT/UFRRJ and was used to evaluate the antimicrobial activity of the silver nanoparticles.

The inoculum suspension (*E. coli*) was prepared through three transfer cultures, from the frozen stock, in Sasoy broth for 25 hours at 36 °C. The bacterial suspension was diluted with peptone water until the turbidity reached an absorbance between 0.1-0.2 in a UV-vis spectrophotometer at λ = 580 nm, which corresponds to 10^9 CFU mL^{-1} (Colony Forming Units) of bacteria concentration. Portions of 10 mg of purified clay, organo-clay, nanocomposites, Ag-MMT purif., and Ag-MMT organ. were sterilized by exposure to UV radiation for 30 minutes. These samples were subsequently added into 250 mL flasks containing sterile tryptone soy broth (180 mL) inoculated with 0.2 mL suspension of *E. coli* at approximately 10^6 CFU mL^{-1}. The flasks were shaken at 150 rpm for 24 hours at 30 °C. After this incubation time, cultures were plated on tryptone soy agar and incubated at 36 °C for 24 hours. Colony counting was performed in duplicate.

3. Results and Discussion

Organic matter has great influence on the exchange capacity of clays; it can act as a protective colloid hampering the exchange of cations [19]. Basal spacing d_{001} values from each sample (Table 1) were calculated using Bragg's Law after the analysis of X-ray diffractograms. We observed increased spacing after the process of purification and modification, thus confirming the efficiency of the applied procedures. The changes represented the replacement of exchangeable ions, present in the clay's galleries by $HDTMA^+$ organic cation and Cetremide; these changes expanded the clay's basal spacing. Thus, a satisfactory differentiation in basal spacing was obtained in the organo-clay (1.41 nm) compared with the commercial clay (1.27 nm).

Table 1. Basal spacings.

Sample	2θ	d_{001} (nm)
Commercial MMT	6,96	1,27
Purified MMT	6,44	1,36
Organophilic MMT	6,26	1,41

X-ray diffractograms showing basal spacing values in the purified and organophilic clay after adsorption of silver cations (Figures 1 and 2, respectively).

The diffractogram (Figure 1) for the purified clay shows reduction in peak intensity (001) with increasing concentrations of silver nitrate. Consequently, the basal spacing, originally 1.36 nm after the purification process, decreased. According to [13], a decrease in the basal intensity diffraction indicates that the lamellar clay has been partially exfoliated due to increased amounts of silver ions in the clay's galleries, causing structural stress during cation exchange. However, the peak intensity in the diffractograms, relative to the 0.1 M $AgNO_3$ concentration, almost completely disappears indicating that exfoliation/delamination definitively occurred in the clay, i.e., the lamellar structure is shown dispersed and disorganized. In contrast, the organo-clay structure was not altered by the increasing concentrations of Ag^+ because the presence of the alkylammonium $HDTMA^+$ ion is retained in the interlayer, causing the clay layers to remain joined and arranged in parallel, thus preventing the effect of exfoliation/delamination. However, [11], who used kaolinite clay interspersed with dimethyl sulfoxide (DMSO), reported that unhindered DMSO is removed from the interlayer space after adsorption of silver ions.

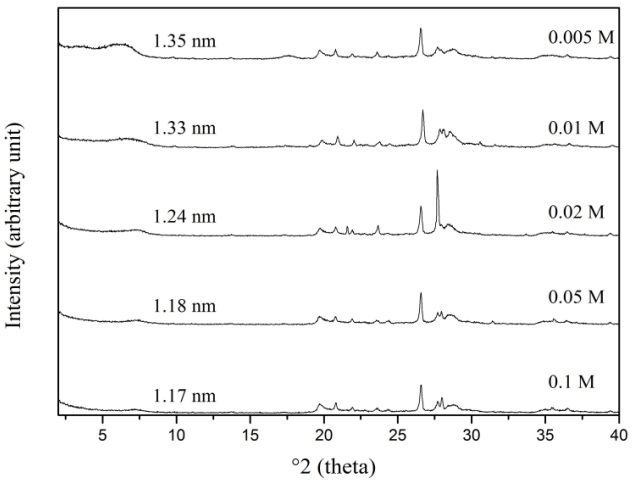

Figure 1. X-ray diffractogram of purified clay intercalated with silver ions at different concentrations of $AgNO_3$ solutions.

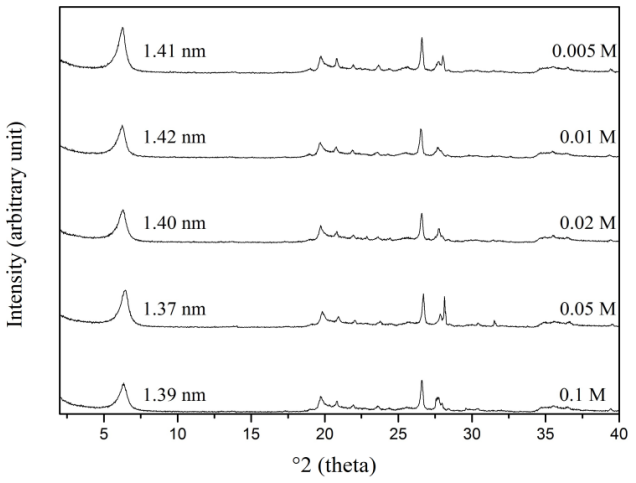

Figure 2. X-ray diffractogram of modified clay intercalated with silver ions at different concentrations of $AgNO_3$ solutions.

The reduction in silver ions adsorbed in the structure of purified and organophilic clay after treatment with $NaBH_4$ was based on the concentration of 0.01 M $AgNO_3$. The reduction method to obtain nanocomposites consisted of adding samples of Ag^+-MMT purif. and Ag^+-MMT org. into in freshly prepared 200 mL $NaBH_4$ solutions at the concentrations of 0.001 M, 0.005 M, and 0.01 M. The reduction of ions present in the purified clay showed a caramel color (the initial solution was colorless) in all $NaBH_4$ concentrations that differed only in grades of transparency. However, the reduction of ions present in the organo-clay showed pale-yellow and light-yellow color, and colorless, solutions at 0.001 M, 0.005 M, and 0.01 M $NaBH_4$, respectively. The color changes confirmed the reduction of silver ions and formation of nanoparticles; agglomeration was also observed. According to [17], caramel coloring clearly indicates increased aggregation of particles in solution, while the yellow coloring shows decreased agglomeration.

Furthermore, the existence of metal nanoparticles was confirmed by the UV-visible spectra (Figures 3 and 4). The caramel colored solutions were diluted 1:10 to ensure stable absorbance readings.

UV-visible spectrophotometry showed reduced peak intensities with increasing $NaBH_4$ concentrations. This means that smaller diameter particles are synthesized at higher $NaBH_4$ concentrations, which favors the adsorption of nanoparticles on the clay's surface. This reduction phenomenon in montmorillonite was described by [24], who reported that metallic silver remains synthesized on the solid phase (montmorillonite) while silver ions are removed from the interlayer, reduced, and adsorbed on the outer surface and edges of the clay.

The colloids produced after silver ion reduction in the purified clay showed a darker color compared with those produced in the organophilic clay. According to what was discussed above, the purified clay shows greater adsorption capacity of silver ions; their reduction increased the concentration of nanoparticles in solution causing a small agglomerative state that was independent of the $NaBH_4$ concentration used. However, the spectra (Figure 4) shows that the amount of nanosized particles in solution was reduced by half at the concentrations of 0.001 M and 0.01 M $NaBH_4$ possibly as the result of increased adsorption of nanoparticles by the organo-clay considering that no agglomeration in the colloid and the formation of smaller size particles were observed.

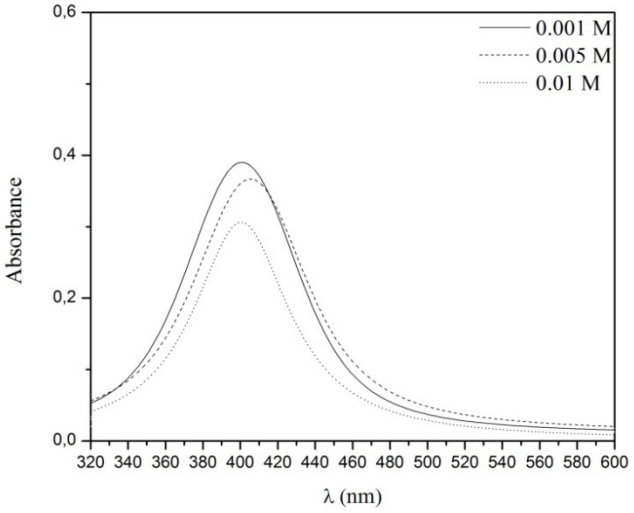

Figure 3. UV-visible spectrophotometry of purified clay supernatants after silver ions reduction using different concentrations of $NaBH_4$.

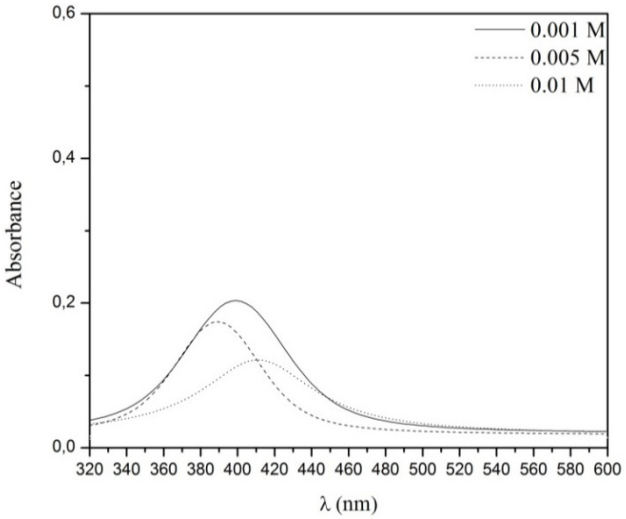

Figure 4. UV-visible spectrophotometry of organo-clay supernatants after silver ions reduction using different concentrations of $NaBH_4$.

The organo-clay structure was not modified by the formation and adsorption of silver nanoparticles in the interlamellar space; therefore, the basal spacing remained similar from the adsorption to the reduction of cations (Figures 5 and 6). However, we observed an increase in basal spacing in the purified clay after reduction with $NaBH_4$ at 0.005 M and 0.01 M. Reference [13] concluded that this expansion occurs because of intercalation of sodium (from the $NaBH_4$ solutions), which provides a restored stacked lamellar structure. Moreover, [12] attributed the increase in

basal spacing to the formation of nanoparticles in the galleries.

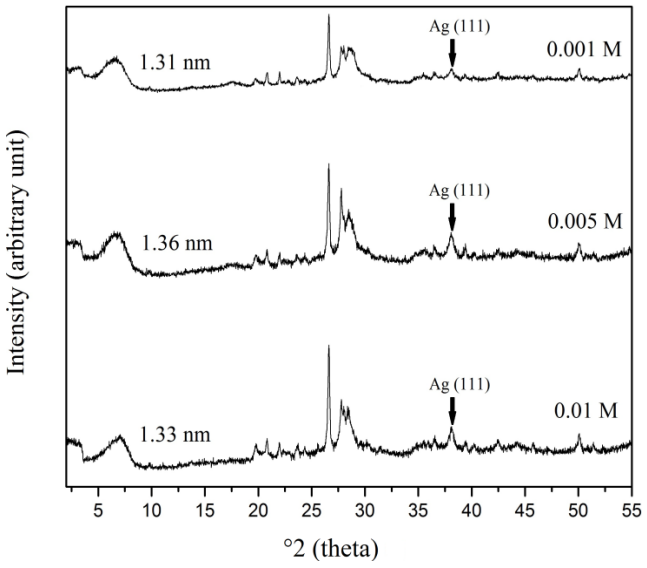

Figure 5. X-ray diffractogram of purified clay after silver ions reduction using $NaBH_4$ solutions.

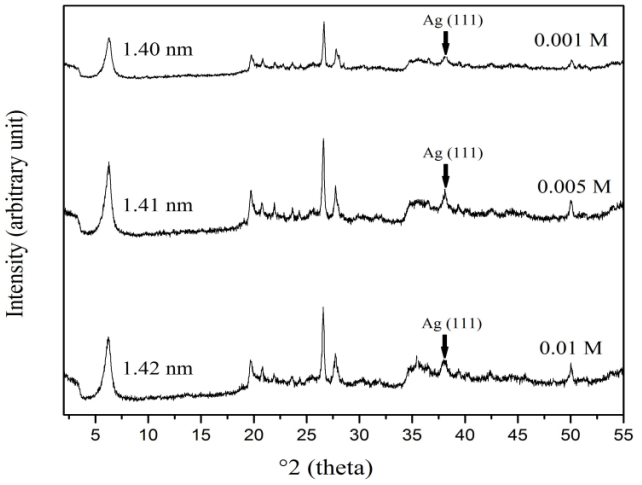

Figure 6. X-ray diffractogram of organo-clay after silver ions reduction using $NaBH_4$ solutions.

All nanocomposites showed diffraction peaks at 2θ of approximately 38°; these peaks are consistent with reflections from the (111) crystallographic planes of face-centered cubic silver. The average size of silver crystallites present in the nanocomposites, obtained by Ag^+ reduction with 0.01 M $NaBH_4$, was calculated using the Scherrer equation because these samples maintained constant basal spacing values after the reduction process. The average silver crystallite size, *D*, was 7.59 nm in the diffraction angle of 38.12° for the Ag-MMT purif. sample, and 7.67 nm in the diffraction angle of 38.02° for the Ag-MMT org. sample.

The bactericidal activity of the produced nanocomposites was tested using *E. coli*. Samples were added to suspensions containing bacteria and incubated for 24 hours to comply with the required time for significant bacterial growth [25]. The positive control consisted of *E. coli* culture in sterile nutrient broth without the addition of samples. The antimicrobial activity (Figure 7) of Ag-MMT purif. and Ag-MMT org. nanocomposites was compared with the organophilic and purified clay. Inhibition of bacteria growth was only observed in the assays with nanocomposites containing silver nanoparticles in their structure.

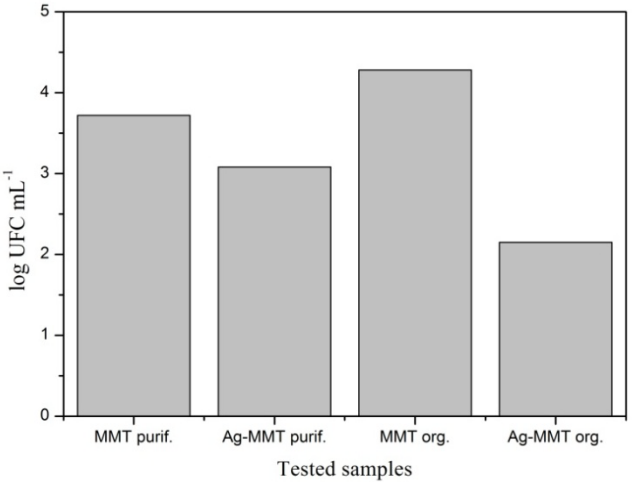

Figure 7. Growth of *E. coli* in the presence of purified MMT, organophilic MMT, Ag-MMT purif., and Ag-MMT org samples.

The mechanism of action of the antimicrobial activity of silver nanoparticles is based on their penetration in the bacteria cell and reaction with thiol and phosphate groups that are present in membrane proteins or enzymes. Therefore, silver nanoparticles bind to the cell membrane inhibiting cellular respiration and division and leading to cell death [3,6].

The Ag-MMT org. sample showed greater antimicrobial activity than the Ag-MMT purif. sample although both samples showed similar nanoparticle sizes on the surface, 7.67 and 7.59 nm, respectively. Therefore, this difference in activity could be related to the reduction of adsorbed Ag^+ in the material. The organo-clay showed fewer nanoparticles aggregates than the purified clay; these less aggregated particles with smaller diameters may be present in the interlamellar space and in greater amounts than the purified clay. According to [26], the reactivity of silver nanoparticles is mainly related to their diameters. The smaller diameter particles provide greater bactericidal activity. However, nanoparticles with a diameter of approximately 5 nm show improved activity against Gram-negative bacteria.

The montmorillonite clay intercalated with cationic surfactants, including cetyl trimethyl ammonium bromide, can also be used as an antimicrobial material [27]. The antibacterial activity in cetyl trimethyl ammonium bromide results from its ability to alter the permeability of cell membranes by allowing ions and intracellular metabolites of low molecular weight to diffuse out of the cell [25]. However, MMT organophilic showed no antimicrobial activity against *E. coli* in the present study. This could have resulted from

diminished antimicrobial activity caused by the quaternary salt intercalated in the montmorillonite structure, compared to its activity as free salt. The greatest bactericidal activity was observed in the assays with Ag-MMT organophilic; this result could be attributed to a possible synergism between the quaternary salt and silver.

4. Conclusions

The modified clay showed a positive result, whereas its structure remained intact through the adsorption and reduction of silver ions. However, the Ag-MMT org. nanocomposite showed greater antimicrobial activity against *E. coli* than Ag.-MMT purif. because the material contained more silver nanoparticles in its structure. Our results demonstrated that the combination of Ag-MMT organo-clay nanocomposite with various types of material is relevant and advantageous for potential industrial applications.

Acknowledgements

The authors are grateful for the financial support from FAPERJ (Fundação Carlos Chagas Filho de Amparo à Pesquisa do Estado do Rio de Janeiro) and the scholarships granted by CAPES and CNPq.

REFERENCES

[1] C. W. Chambers, C. M. Proctor, P. W. Kabler, Journal of American Water Works Association, (1962) 208.

[2] J. P. Guggenbichler, M. Boswald, S Lugauer, T. Krall, Infection 27 (1999) 16.

[3] R. Dastjerdi, M. Montazer, Colloids and Surfaces B: Biointerfaces 79 (2010) 5.

[4] K. Shameli, M. B. Ahmad, W. M. Z. W. Yunus, N.A. Ibrahim, Y. Gharayebi, S. Sedaghat, International Journal of Nanomedicine 5 (2010) 1067.

[5] Huan, H., and Yang, Y. (2008) Preparation of silver nanoparticles in inorganic clay suspensions. Composites Science and Technology, 68, 2948-2953.

[6] A. I. Incoronato, G. G. Buonocore, A. Conte, M. Lavorgna, M. A. Nobile, Journal of Food Protection 73 (2010) 2256.

[7] A. Oya, T. Banse, F. Ohashi, S. Otani, Applied Clay Science 6 (1991) 135.

[8] J. Tokarský, P. Čapková, V. Klemm, D. Rafaja, J. Kukutschová, Journal of Physics and Chemistry of Solids 71 (2010) 634.

[9] I. Pastoriza-Santos, L. M. Liz-Marzan, Pure and Applied Chemistry 72 (2000) 83.

[10] S. Komarneni, D. Li, B. Newalkar, H. Katsuki, A. S. Bhalla, Journal Langmuir 18 (2002) 5959.

[11] R. Patakfalvi, A. Oszkó, I. Dékány, Colloids and Surfaces A: Physicochemical and Engineering Aspects 220 (2003) 45.

[12] M. B. Ahmad, K. Shameli, M. Darroudi, W. M. Z. W. Yunus, N. A. Ibrahim, American Journal of Applied Sciences 6 (2009) 1909.

[13] P. Praus, M. Turicová, M. Valášková, Journal of the Brazilian Chemical Society 19 (2008) 549.

[14] Z. S. Pillai, P. V. Kamat, The Journal of Physical Chemistry B, 108 (2004) 945.

[15] L. Suber, I. Sondi, E. Matijević, D. V. Goia, Journal of Colloid and Interface Science 288 (2005) 489.

[16] P. Praus, M. Turicová, M. Klementová, Journal of the Brazilian Chemical Society, 20 (2009) 1351.

[17] S. Solomon, M. Bahadory, A. Jeyarajasingan, S. Utkowsky, C. Boritz, Journal of Chemical Education 84 (2007) 322.

[18] W. R. Caseri, Materials Science and Technology 22 (2006) 807.

[19] P. S. *Santos*, *Ciência e Tecnologia* de Argilas, Edgard Blucher Ltda, São Paulo, *(1989)* 2nd ed.

[20] H. van Olphen, An Introduction to Clay Colloid Chemistry, John Wiley & Sons, New York. (1977) 2nd ed.

[21] S. A. Boyd, S. Shaobai, J. F. Lee, M. M. Mortland, Clays and Clays Minerals 36 (1998) 125.

[22] G. L. V. Coelho, F. Augusto, J. Pawliszyn, Industrial & Engineering Chemistry Research 40 (2001) 364.

[23] J. I. Langford, A. J. C. Wilson, Journal of Applied Crystallography 11 (1978) 102.

[24] M. Valášková, G. S. Martynková, J. Lešková, P. Čapková, V. Klemm, D. Rafaja, Journal Nanoscience and Nanotechnology 8 (2008) 3050.

[25] K. Malachová, P. Praus, Z. Pavlíčková, M. Turicová, Applied Clay Science 43 (2009) 364.

[26] J. R. Morones, J. L. Elechiguerra, A. Camacho, K. Holt, J. B. Kouri, J. T. Ramirez, M. J. Yacaman, Nanotechnology 16 (2005) 2346.

[27] P. Herrera, R. Burghardt, H. J. Huebner, T. D. Phillips, Food Microbiology, 21 (2004) 1.